



Effect of vacuum annealing on the structural and optical properties of sputtered Cu_4O_3 thin films

L. Radjehi, L. Aissani, A. Djelloul, S. Lamri, K. Nomenyo, S. Achache, G. Lerondel & F. Sanchette

To cite this article: L. Radjehi, L. Aissani, A. Djelloul, S. Lamri, K. Nomenyo, S. Achache, G. Lerondel & F. Sanchette (2020): Effect of vacuum annealing on the structural and optical properties of sputtered Cu_4O_3 thin films, Surface Engineering, DOI: [10.1080/02670844.2020.1753397](https://doi.org/10.1080/02670844.2020.1753397)

To link to this article: <https://doi.org/10.1080/02670844.2020.1753397>



Published online: 29 Apr 2020.



Submit your article to this journal [↗](#)



View related articles [↗](#)



View Crossmark data [↗](#)



Effect of vacuum annealing on the structural and optical properties of sputtered Cu_4O_3 thin films

L. Radjehi^a, L. Aissani^b, A. Djelloul^a, S. Lamri^c, K. Nomenyo^d, S. Achache^c, G. Lerondel^d and F. Sanchette^{c,e}

^aLaboratoire des structures, propriétés et interactions inter atomiques (LASPI2A), Faculty of Science and Technology, Abbes Laghrour University, Khenchela, Algeria; ^bLaboratory of Active Components and Materials, Larbi Ben M'Hidi University, Oum El Bouaghi, Algeria; ^cLaboratoire des Systèmes Mécaniques et d'Ingénierie Simultanée, Institut Charles Delaunay, CNRS, Université de Technologie de Troyes (UTT), Nogent, France; ^dLight, Nanomaterials, Nanotechnologies (L2N, former LNIO), Institut Charles Delaunay, CNRS, Université de Technologie de Troyes (UTT), Troyes, France; ^eNogent International Center for CVD Innovation, LRC CEA-ICD LASMIS, UTT, Antenne de Nogent-52, Pôle Technologique de Haute-Champagne, Nogent, France

ABSTRACT

Cu_4O_3 thin films were deposited by the reactive magnetron sputtering process on glass and Si (100) wafers. In order to investigate the thermal stability of the Cu_4O_3 phase, the films were subjected to vacuum annealing treatment for one hour at various temperatures ranging from 200°C to 500°C. The samples were characterized by using EDS, XRD, SEM and UV-VIS. The phase transformation of Cu_4O_3 into Cu_2O was obtained from 300°C (critical temperature). Increasing annealing temperature leads to compact morphology and the grain shape changing from elongated towards spherical. Due to this annealing the film structure presents coexistence of a Cu_4O_3 and Cu_2O mixture where O atoms are lost in the Cu-O system. The UV-VIS analysis reveals a gradual increase in the transmittances from 55 to 70% with the increasing annealing temperature, while the band gap shows a maximum value ($E_g = 2$ eV) at 500°C corresponding to the Cu_2O phase.

ARTICLE HISTORY

Received 3 April 2019
Revised 1 March 2020
Accepted 21 March 2020

KEYWORDS

Cu_4O_3 ; Cu_2O ; annealing treatment; critical temperature; transmittance; band gap; thermal stability; thin films

Introduction

Paramelaconite (Cu_4O_3) with exclusive oxygen saturation has received a large technological interest in various field applications like photovoltaic, catalysis, lithium storage batteries and solar cells [1–7]. Cu_4O_3 is a metastable phase that has copper atoms in two valence state: Cu^{I} and Cu^{II} [1]. Thus, few research studies have devoted to study the properties of Cu_4O_3 thin films. Koenig et al. have determined its composition and crystal class as they named it melaconite [2]. Next, O'Keeffe and Bovin found that the Cu_4O_3 composition should be presented by $\text{Cu}(\text{I})_2\text{Cu}(\text{II})_2\text{O}_3$ [3,4]. Hsueh et al. have deposited Cu_4O_3 nanowires by using magnetron sputtering to develop $\text{Cu}_4\text{O}_3/\text{ZnO}$ photodiodes [5]. Recently, H.S. Kim et al. have elaborated devices based on Cu_4O_3 for photodetector applications [8]. However, the use of Cu_4O_3 thin films in various applications needs a good quality of materials, in terms of structural, optical and electrical properties. The enhanced properties of Cu_4O_3 films can be achieved by changing the microstructure and chemical composition. This is typically controlled by the deposition parameters and the applied treatment. Knowing that Cu_4O_3 is a metastable phase, heat treatment influences their structure properties. Therefore, vacuum and air annealing can transform Cu_4O_3 into Cu_2O or CuO . Pierson et al. have

studied the thermal stability in air of the different copper oxide films at 300°C, 350°C and 400°C during 4 h. They found that the thermal conversion of Cu_2O and Cu_4O_3 into CuO with an increase of the resistivity with a slight decrease of a stable CuO phase at the same temperature (350°C) [7]. D.S. Murali et al. have studied the effect of the thermal treatment on Cu_4O_3 films by using the high-temperature Raman analysis. They found that the transition of Cu_4O_3 to the CuO phase after annealing of the Cu-O films at 410°C and 450°C in ambient air and argon atmosphere, respectively [9]. Vacuum annealing of Cu-O films shows enhanced electrical and optical properties for Cu_2O thin films [10].

However, only limited reports on sputtered Cu-O films are available; these are either discussing the thermal stability of Cu_4O_3 in vacuum annealing [10], or the influence of oxygen content on the optical and electrical properties without comprehensive information on the chemical and structural properties [9]. The major advantage of vacuum annealing is that it provides uniformity in the structure due to the atoms' rearrangement without oxygen insertion [11].

In this paper, we have deposited the Cu_4O_3 thin films using DC magnetron sputtering. Then, the films were annealed under vacuum at different temperatures from 200°C to 500°C. The aim of this work is to study the Cu_4O_3 thermal stability and to investigate the

correlation between heat treatment and structural properties. The impact of vacuum annealing on the optical behaviour, especially the band gap of each phase as well as that of the mixture ($\text{Cu}_4\text{O}_3 + \text{Cu}_2\text{O}$), was also studied.

Experimental and details

Film deposition

Cu_4O_3 films were deposited by a DC magnetron sputtering process in a reactive mode (Alcatel SCM600) at a total working pressure ($\text{Ar} + \text{O}_2$) of 0.5 Pa and a Cu discharge current of 1A. The Cu target (99.9% purity, 200 mm diameter) was fixed on a magnetron-effect cathode. The substrate holder was situated in front of the target at 140 mm distance and with an angle of 90° from the normal, to obtain films uniform thickness. The details of the deposition conditions used in this work have been reported in the literature [11]. Before the deposition procedure, the process chamber was evacuated to a vacuum of 10^{-4} Pa.

The substrates ($2.5 \times 2.5 \text{ cm}^2$) and Si(100) wafers ($1 \times 1 \text{ cm}^2$) were cleaned in an ultrasonic bath of acetone and ethanol solution for 5 min for each one. Thereafter, the substrates and targets were cleaned by Ar ion etching for 5 min and surface oxide layers or impurities were removed. The cleaning step was performed with the following conditions: argon flow rate of 50 sccm, pressure of 0.4 Pa, voltage of 450 V, power of 230 W.

Cu–O films were deposited by adjusting the voltage (power) of Cu target at 500 V (250 W) and using a constant working pressure at 0.5 Pa during 40 min in O_2 (25 sccm) plus Ar (50 sccm) gas mixture. The floating temperature was 68°C during the deposition process.

Thermal treatment

Cu_4O_3 films were annealed under vacuum at various temperatures (200°C , 250°C , 300°C , 350°C , 400°C , 450°C , 500°C) in a tubular furnace. The thermal cycle consisted of a ramp of $10^\circ\text{C min}^{-1}$, followed by maintaining at the desired temperature for 1 h. Finally, the cooling takes place under vacuum at a rate of about $-10^\circ\text{C min}^{-1}$. A diffusion pump insured the pressure of 10^{-7} Pa.

Film characterization

Film composition was determined by the Bruker electron probe X-ray micro-analyzer. The Cu_4O_3 crystalline structure was analysed by X-ray diffraction (XRD) using a D8 advanced with a $\text{Cu}_{K\alpha}$ radiation source (40 kV, 40 mA, $\lambda_{\text{Cu}} = 0.154 \text{ nm}$). The crystallite size (D) was estimated from the full width at half-

maximum of the (002), (400) and (004) of Cu_4O_3 phase and (111) Cu_2O orientations using the Scherrer's formula [12]:

$$D = \frac{0.94\lambda}{\beta \cos \theta} \quad (1)$$

where 0.94 is a shape factor, λ represents the X-ray wavelength of the radiation source used for the measurement ($\lambda_{\text{Cu}} = 0.154 \text{ nm}$), β (rad) is the line full width at half-maximum and θ is the Bragg's angle.

The lattice parameter (c) for each orientation on the Cu_4O_3 tetragonal phase was determined by the inter-reticular equation:

$$d_{hkl} = \frac{ac}{\sqrt{c^2(h^2 + k^2) + a^2l^2}} \quad (2)$$

In addition, the Cu_2O cubic phase was evaluated by

$$d_{hkl} = \frac{a}{\sqrt{h^2 + k^2 + l^2}} \quad (3)$$

The microstrains of Cu_4O_3 or Cu_2O phases were calculated using the following equation:

$$\varepsilon = \frac{\Delta d}{d_{\text{bulk}}} \quad (4)$$

where ε is the microstrain in the direction of the c axis, i.e. perpendicular to the substrate surface $\Delta c = c_{\text{film}} - c_{\text{bulk}}$, d_{film} and d_{bulk} of Cu_4O_3 or Cu_2O phases.

The cross-section and the surface morphologies were observed by using a field emission scanning electron microscope (FE-SEM-Hitachi-SU8030).

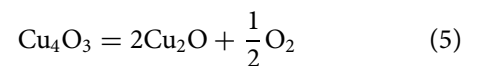
The average roughness Ra was measured with an atomic force microscope (AFM 100, APE research), which was employed under contact mode with the scan range of $3 \times 3 \mu\text{m}$.

The transmittance of the annealed Cu_4O_3 films was measured by using a Perkin Elmer UV–VIS Lambda 19 spectrophotometer in the 190–1100 nm spectral range.

Results and discussion

Structure and chemical composition

The Cu_4O_3 and Cu_2O phases differ from each other in the stoichiometric ratio. The reduction of Cu_4O_3 to Cu_2O is governed by the endothermic reaction [13]:



Thus, energy from a vacuum annealing is needed to convert the Cu_4O_3 into Cu_2O .

The O/Cu atomic ratio of the as-deposited film was found to be 3/4. However, the increase of vacuum annealing temperature leads to a drop in the O/Cu atomic ratio down to 1/2 at 500°C . According to Sun H. et al., the increase of annealing temperature caused

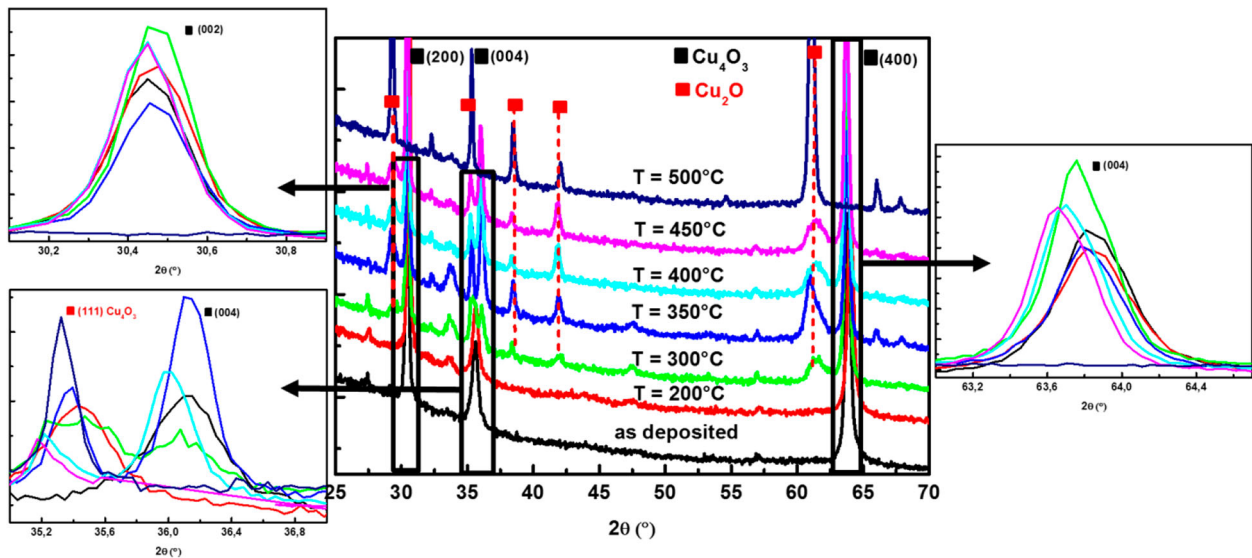


Figure 1. XRD evolution of copper oxides films at different vacuum annealing temperatures.

the movement of oxygen atoms out of the Cu crystal lattices and the formation of copper oxide compounds with low oxygen content [14]. This is due to the relative reduction of oxygen during vacuum annealing treatment.

Figure 1 presents the XRD patterns of Cu_4O_3 films (960 nm thick) before and after vacuum annealing treatments. Before vacuum annealing, the films revealed peaks at 30.96° , 36.11° and 61.26° , corresponding to (200), (004) and (400) crystallographic orientation of the tetragonal Cu_4O_3 phase (JCPDS Card # 49-1830). Below 300°C , the same peaks were observed, this indicates that no phase transformation occurred. J.F. Pierson et al. found the same structure by using the RF magnetron sputtered Cu_4O_3 films [15]. Between 350°C and 450°C , new weak peaks (110), (111) and (220) have appeared at 29.55° , 36.42° and 61.34° , corresponding to the cubic Cu_2O phase (JCPDS Card # 5-0667). In our case, XRD analysis confirms the total transformation of Cu_4O_3 to Cu_2O at 500°C . The disappearance of the Cu_4O_3 phase is observed and the Cu_2O phase becomes dominated by the appearance of the predominant (111) peak at 500°C that confirms the total transformation of Cu_4O_3 to Cu_2O . Similar behaviour was observed by J. Sohn et al., which found that the transformation of the monoclinic CuO into cubic Cu_2O is accelerated at higher temperatures (at 500°C) by the reducing

process [16–18]. Blobaum et al. found that Gibbs free energy of Cu_4O_3 formation is $-40 \text{ kJ} \cdot (\text{mol atom})^{-1}$, which is less than that of Cu_2O ($-39.22 \text{ kJ} \cdot (\text{mol atom})^{-1}$), indicating the thermodynamic instability of bulk Cu_4O_3 at elevated temperatures [19]. Therefore, 300°C is the critical temperature of phase transformation of Cu_4O_3 under vacuum annealing.

Residual microstrains (ϵ) of Cu_4O_3 films as a function of annealing temperature are presented in Table 1. All films are in compressive stress state. The increasing temperature leads to the gradual decrease in the microstrains from -0.365 (before annealing) to -0.0812% (at 500°C). This may be attributed to the relaxation of the stresses and the decrease in the Cu_4O_3 lattice parameter that is the result of the thermal treatment [11].

Figure 2 shows the full width at half-maximum (FWHM) and the peaks shift as a function of annealing temperature for Cu–O films. These results were obtained for both Cu_4O_3 and Cu_2O phases. Increasing the annealing temperature obviously leads to a significant increase in the increase of FWHM and peaks shift.

These changes in Cu_4O_3 FWHM and peaks positions suggest that the relaxation of the Cu_4O_3 lattice follows progressively as the oxygen content in the films decreases. Loss of oxygen leads to a progressive conversion of Cu_4O_3 phase to Cu_2O , resulting in a severe decrease in intensity that accompanied with an

Table 1. Evolution of d_{hkl} and microstrains of Cu_4O_3 and Cu_2O phases as a function of annealing temperatures.

T(°C)	(Cu_4O_3) d_{200}	(Cu_4O_3) d_{004}	(Cu_4O_3) d_{400}	(Cu_2O) d_{111}	E (%)
As-deposited	2.933	2.848	1.5500	/	0.242
200	2.922	2.845	1.5510	/	0.181
300	2.919	2.844	1.5498	2.456	-0.365
350	2.914	2.833	1.5482	2.459	-0.243
400	2.915	2.835	1.5486	2.460	-0.203
450	2.916	2.838	1.5489	2.461	-0.162
500	/	/	/	/	-0.081

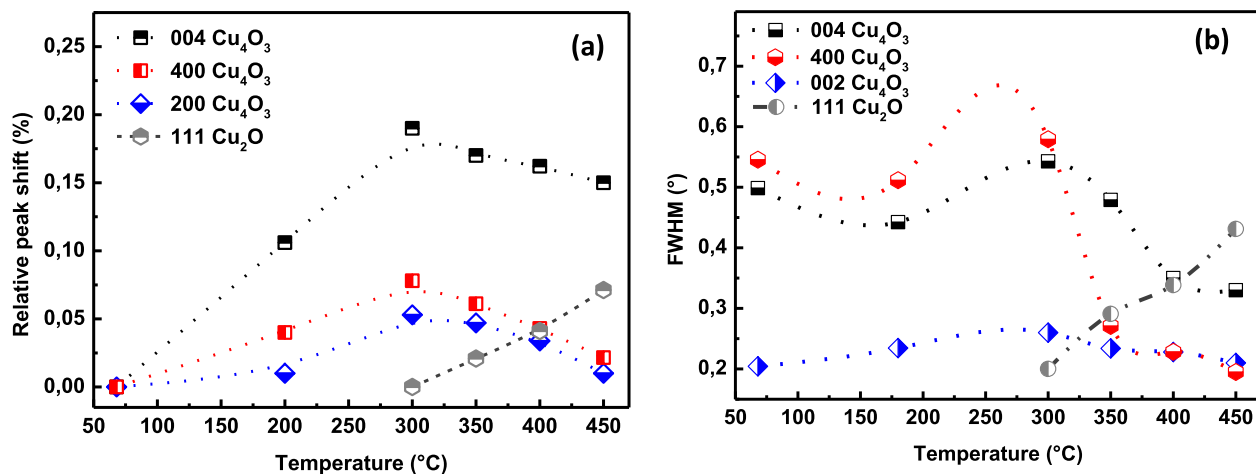


Figure 2. (a) Relative shift, (b) FWHM of (200), (004) and (400) Cu_4O_3 and (111) Cu_2O peaks at different vacuum annealing temperatures.

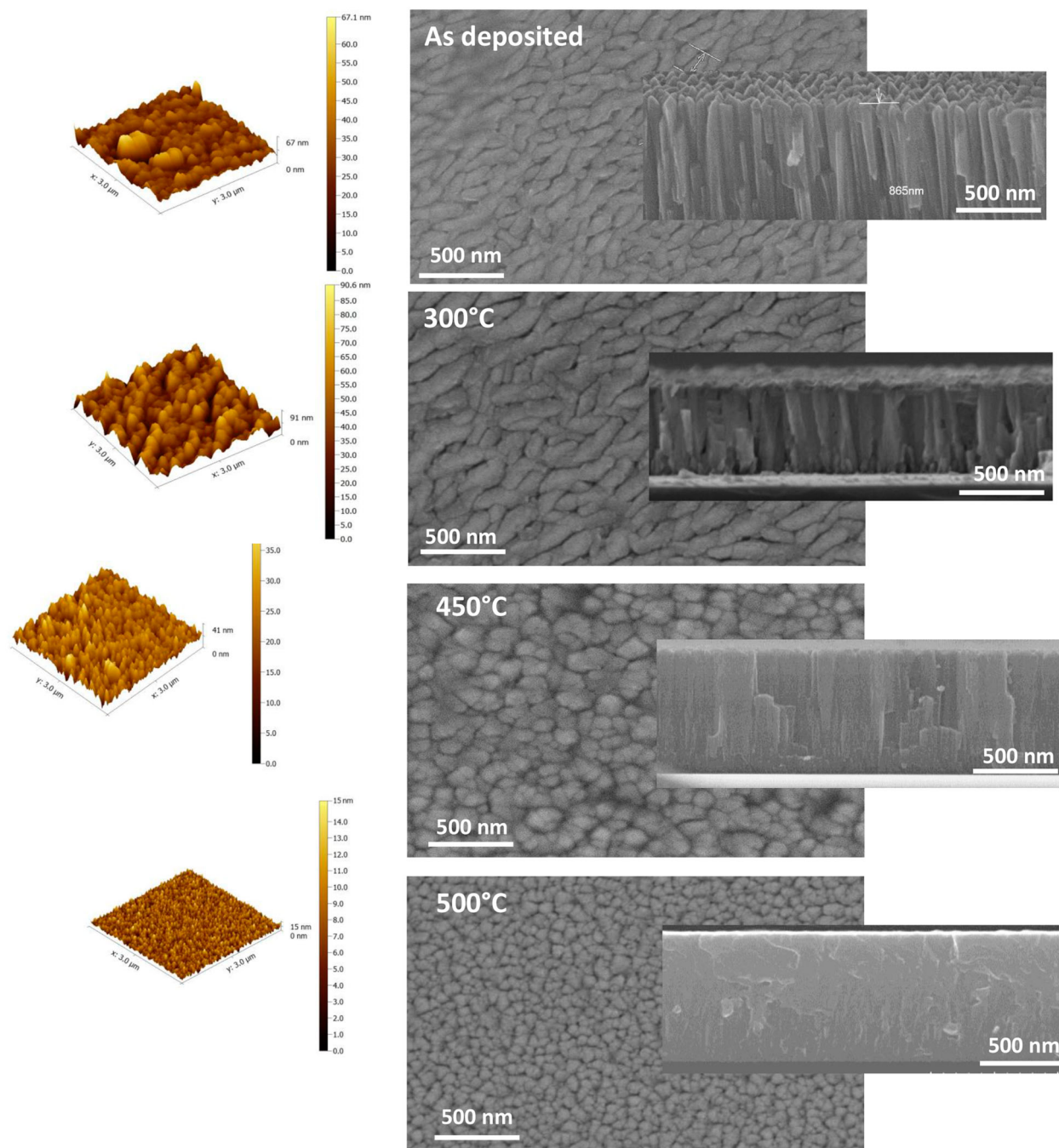


Figure 3. Top-view and cross-section SEM images and AFM topography of Cu_4O_3 as-deposited heated thin films at different vacuum annealing temperatures.

Table 2. Evolution of crystallite size as a function of annealing temperatures.

Cryst size (nm)/T(°C)	(200)Cu ₄ O ₃	(004)Cu ₄ O ₃	(400)Cu ₄ O ₃	(111)Cu ₂ O
As-deposited	30.82	17.96	18.59	/
200	34.76	19.02	19.92	/
300	32.21	35.65	23.34	33.71
350	36.57	38.14	21.81	29.34
400	37.83	36.71	20.34	28.33
450	36.74	34.65	20.09	27.76
500	/	/	/	15.28

increase in FWHM of the (111) Cu₂O. This is due to the poor crystallization of Cu₄O₃ and the relatively low oxygen content in the film. Film structure evolution is related to the compressive microstrains introduced in the film, during annealing treatment, via the complex nature of reaction between copper and oxygen atoms [11,17].

Below 300°C, the XRD peaks of the tetragonal Cu₄O₃ phase slightly shift to higher diffraction angles, suggesting a small lattice distortion (Figure 2(a)). From 300°C to 500°C, XRD peaks shift to lower diffraction angles that indicate the increase of lattice parameter. This is explained by increasing microstructural strain or crystallite size effects in the film [17].

Figure 3 shows the FESEM and the AFM images of Cu₄O₃ films deposited on silicon substrates. It is obvious that the morphology of the deposited film depends on annealing temperature. Before vacuum annealing, the film surface presents homogenous elongated grains with a mean crystallite size of 20 nm (Table 2). At 300°C, the film shows the same grain shape as before vacuum annealing, with the enlargement of grain size, indicating an improvement in crystallinity.

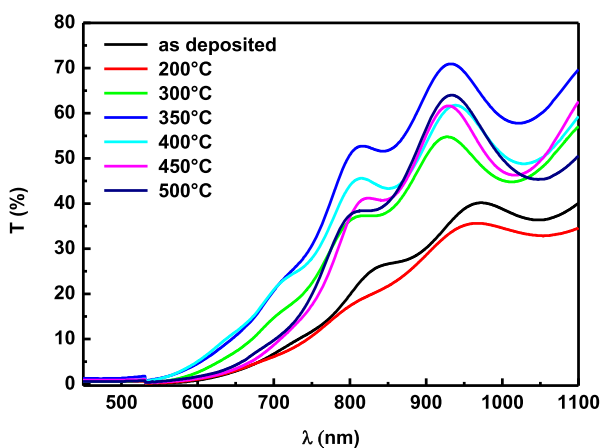
Before annealing, the Cu₄O₃ film exhibits a dense columnar structure with elongated grains, which is a result of high working pressures (0.5 Pa) (Figure 3). The crystallite size and the roughness are 19 nm. Moreover, the AFM topography of the Cu–O films has

coarse irregular tops surrounded by large voids with large grains and high roughness (67.1 nm). Similar morphology evolution has been reported in the literature [11,18]. At 300°C, the film presents the same grain morphology as before vacuum annealing, with a grain size enlargement. The mean crystallite size and the film roughness of the Cu₄O₃ films are clearly increased (31 and 90.6 nm), respectively. Above 300°C, temperature increasing leads to the changing in the structure. At 450°C, the films exhibit more compact morphology than that of as-deposited films. The grain becomes spherical like form, which corresponds to the Cu₂O phase [9]. These grains become finer at 500°C with a crystallite size of 25 nm. Thus, the grains (Ra = 15 nm) become smooth and homogeneous tops with small voids that might be due to recrystallization of the films [15,16].

Optical property

Figure 4 shows the UV–VIS spectra of Cu₄O₃ films, before and after annealing treatment, at different temperatures. As-deposited and 200°C annealed paramelacornite films show an average transmittance of 38%. An average transmittance of 55% is observed in the film annealed at 300°C. However, between 350°C and 450°C, the films that consist of a mixture of Cu₄O₃ + Cu₂O phases show an average transmittance of 66%. At 500°C, the film that has been completely transformed to Cu₂O, as confirmed by the XDR analysis, shows an improvement on the transmittance, reaching a maximum value of 70%. This enhancement in the transmittance is probably due to the crystallinity improvement [19]. In our case, vacuum annealing between 200°C and 500°C leads to the atom rearrangement of copper oxide structure. Temperature increase leads to larger grain size, as shown in Figure 3. The mechanism that can improve the transmittance properties is the reduction of grain-boundary scattering linked to the larger grain size of the film annealed at high temperature (Figure 5). Generally, the transmittance related to grain-boundary scattering in polycrystals is affected by the porosity, growth orientation and grain size. A low porosity means little scattering at pores. As the refractive indexes are dependent on grain orientations in some material, the refraction at the grain boundaries with different growth orientations will enhance, consequently the reduction of transmittance. Besides, at a given sample thickness, the small grain size will decrease the transmittance, as the light has to pass an increasing number of grain boundaries [20].

The value of the absorption coefficient for the strong absorption region of the thin film is determined by using the equation shown in reference [21]. The band gap energy of the annealing films was evaluated from the plot of $(\alpha hv)^2$ as a function of the photon energy (hv) at the absorption edge of $\alpha = 0$. The values of

**Figure 4.** Optical transmittance spectra of the Cu–O thin films at different vacuum annealing temperatures.

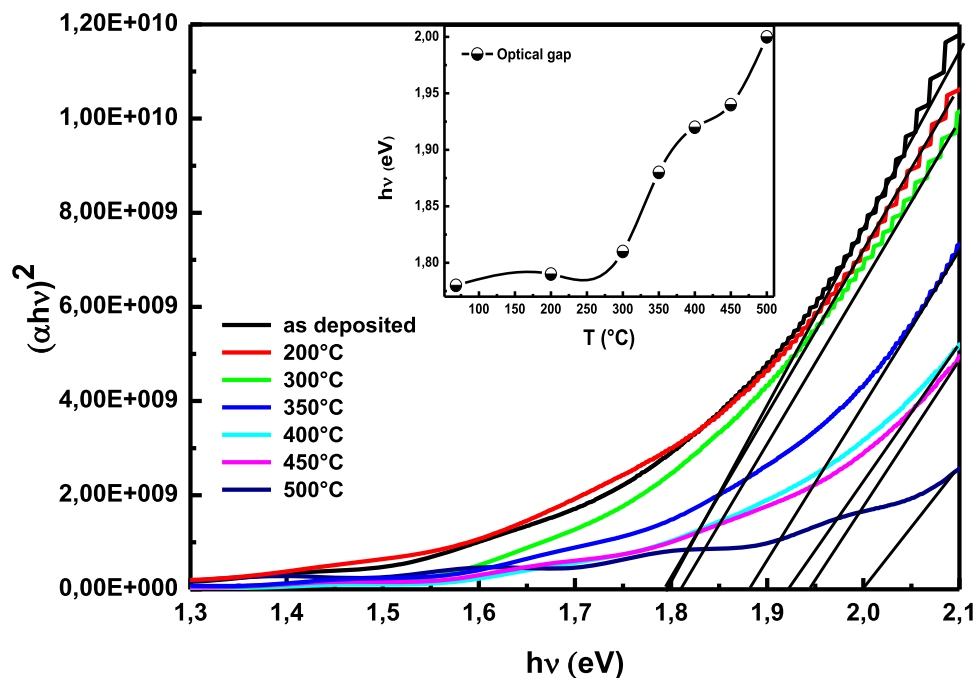


Figure 5. The plots of $(\alpha hv)^2$ vs. hv of Cu–O films (960 nm) at different vacuum annealing temperatures.

the band gap (E_g), as a function of the vacuum annealing temperature, are shown in Figure 5. Below 300°C, the Cu_4O_3 films have an optical gap of 1.85 eV, which corresponds to the Cu_4O_3 phase. W. Zheng et al. found that Cu_4O_3 has an optical gap of 1.65 eV, which is lower than that of our result because of the improvement in the thin film crystallinity with annealing temperature [22]. From 350°C, the optical gap values take a value of 2 eV, which corresponds to the optical gap of the Cu_2O phase [23]. It can be seen that the band gap $8(E_g)$ value (~ 1.9 eV) of the $\text{Cu}_4\text{O}_3 + \text{Cu}_2\text{O}$ mixture phase is ranging between that of Cu_4O_3 (1.8 eV) and Cu_2O (2 eV). Whatever the phase formed as a function of temperature, optical gap increase is observed.

Conclusion

The effect of vacuum annealing treatment 500°C, on the morphological, structural and optical properties of Cu_4O_3 thin films deposited at 0.5 Pa by DC reactive magnetron sputtering, was investigated. The study of the thermal stability of Cu_4O_3 films allows us to highlight the following points.

The Cu_4O_3 phase is stable below 300°C, with an increase in mean grain size and decrease in microstrains. $\text{Cu}_4\text{O}_3 + \text{Cu}_2\text{O}$ phases mixture is found at a temperature ranging between 300°C and 450°C and a total transformation of Cu_4O_3 to Cu_2O is obtained at 500°C.

As-deposited Cu–O films exhibit a dense columnar structure with elongated grains that become fine with spherical shape at 500°C, which corresponds to Cu_2O . The increasing temperature leads to an

improvement in the transmittance from 38% before annealing until 70% at 500°C.

A vacuum annealing was carried out to improve the optical property of Cu–O films; a high band gap value ($E_g = 1.8$ eV) of the Cu_4O_3 phase was obtained after vacuum annealing below 300°C.

Disclosure statement

No potential conflict of interest was reported by the author(s).

References

- [1] Medina-Valtierra J, Frausto-Reyes C, Camarillo-Martinez G, et al. Complete oxidation of isopropanol over Cu_4O_3 (paramelaconite) coating deposited on fiberglass by CVD. *Appl Catal A General*. 2008;356:36–42.
- [2] Koenig GA. On paramelaconite and the associated minerals. *Proc Acad Nat Sci Philadelphia*. 1891;248:84–291.
- [3] O’Keeffe M, Bovin JO. The crystal structure of paramelaconite Cu_4O_3 . *Am Mineral*. 1978;63:180–185.
- [4] Anderson AY, Bouhadana Y, Barad HN, et al. Quantum efficiency and band gap analysis for combinatorial photovoltaics: sorting activity of Cu–O compounds in all-oxide device libraries. *ACS Comb Sci*. 2014;16:53–65.
- [5] Hsueh HT, Chang SJ, Weng WY, et al. Fabrication and characterization of coaxial p-copper oxide/n-ZnO nanowire photodiodes. *IEEE Transactions Nanotech*. 2011;11:127–133.
- [6] Wu X, Liu J, Huang P, et al. Engineering crystal orientation of p- Cu_2O on heterojunction solar cells. *Surf Eng*. 2017;33:542–547. doi:10.1080/02670844.2017.1288342.

- [7] Billard A, Pierson JF, Thobor A. Cuprite, paramelaconite and tenorite films deposited by reactive magnetron sputtering. *App Surf Sci.* **2003**;210:359–367.
- [8] Kim HS, Kumar MD, Park WH, et al. Cu_4O_3 -based all metal oxides for transparent photodetectors. *Sens Actuators A Phys.* **2017**;253:35–40.
- [9] Murali DS, Aryasomayajula S. Thermal conversion of Cu_4O_3 into CuO and Cu_2O and the electrical properties of magnetron sputtered Cu_4O_3 thin films. *App Phys A.* **2018**;3:124–279. doi:10.1007/s00339-018-1666-6.
- [10] Murali DS, Kumar S, Choudhary RJ, et al. Synthesis of Cu_2O from CuO thin films: optical and electrical properties. *AIP Adv.* **2015**;7:047143–047148.
- [11] Radjehi L, Djelloul A, Lamri S, et al. Oxygen effect on structural and optical properties of zinc oxide. *Surf Eng.* **2018a**;34:1–8. doi:10.1080/02670844.2018.1515842.
- [12] Aissani L, Nouveau C, Walock MJ, et al. Influence of vanadium on structure, mechanical and tribological properties of CrN coatings. *Surf Eng.* **2015**;31:779–788.
- [13] Radjehi L, Djelloul A, Bououdina M, et al. Structural and magnetic properties of copper oxide films deposited. *App Phys A.* **2018b**;124(723):723–728. doi:10.1007/s00339-018-2141-0.
- [14] Sun H, Chen SC, Wen CK, et al. p-type cuprous oxide thin films with high conductivity deposited by high power impulse magnetron sputtering. *Ceram Int.* **2017**;43:6214–6220.
- [15] Pierson JF, Duvergerb E, Banakhc O. Experimental and theoretical contributions to the determination of optical properties of synthetic paramelaconite. *J Solid State Chem.* **2007**;180:968–973.
- [16] Sohn J, Song S H, Nam D W, et al. Effects of vacuum annealing on the optical and electrical properties of p-type copper-oxide thin-film transistors. *Semicond Sci Technol.* **2013**;28.
- [17] Kim JY, Rodriguez JA, Hanson JC, et al. Reduction of CuO and Cu_2O with H_2 : H embedding and kinetic effects in the formation of suboxides. *J Am Chem Soc.* **2003**;12535:10684–10692. doi:10.1021/ja0301673.
- [18] Wisz G, Sawicka-Chudy P, Potera P, et al. Morphology, composition, structure and optical properties of thermally annealed Cu_2O thin films prepared by reactive DC sputtering method. *Molecular Cryst Liquid Cryst.* **2019**;672(1):81–91. doi:10.1080/15421406.2018.1542110.
- [19] Blobaum KJ, Heerden DV, Wagner AJ, et al. Sputter-deposition and characterization of paramelaconite. *J Mater Res.* **2003**;18:1535–1542. doi:10.1016/j.egypro.2012.07.008.
- [20] Wang1 Y, Miska1 P, Pilloud D, et al. Transmittance enhancement and optical band gap widening of Cu_2O thin films after air annealing. *J App Phys.* **2014**;115:073505–073510. doi:10.1063/1.4865957.
- [21] Wang B, Xie Y, Yang T, et al. Synthesis and photocatalytic properties of flexible Cu_2O thin film. *Surf Eng.* **2019**;35:1–7.
- [22] Zheng W, Chen Y, Peng X, et al. The phase evolution and physical properties of binary copper oxide thin films prepared by reactive magnetron sputtering. *Materials (Basel).* **2018**;11:1253.
- [23] Husnaa J, Aliyu MM, Islama MA, et al. Influence of annealing temperature on the properties of ZnO thin films grown by sputtering energy. *Energy Procedia.* **2012**;25:55–61.